Supplementary Material: Stepping Stone Mechanism: Carrier-Free Long-Range Magnetism Mediated by Magnetized Cation States in Quintuple Layer*

Chunkai Chan(陈俊佳), Xiaodong Zhang(张小东), Yiou Zhang(张异欧), Kinfai Tse(谢建辉), Bei Deng(邓贝), Jingzhao Zhang(张璟昭), and Junyi Zhu(朱骏宜)**

Department of Physics, Chinese University of Hong Kong, Hong Kong SAR, China

*Supported by Chinese University of Hong Kong (CUHK) (Grant No.4053084), University Grants Committee of Hong Kong (Grant No. 24300814), and start-up funding of CUHK.

**Email: jyzhu@phy.cuhk.edu.hk

Text A: Computational Methods and Details

All calculations are performed using projected augmented wave (PAW) [1] potentials with Perdew-Burke-Ernzerhof (PBE) [2] generalized gradient approximation (GGA) as implemented in Vienna *ab initio* simulation package (VASP) [3]. The cutoff energy for plane-wave expansion was set to 350eV for both Bi_2Se_3 and Bi_2Te_3 and 400eV for Sb_2Te_3. Gamma centered 3×3×1 *k* mesh is used to sample the Brillouin zone for 4×4 supercell of Bi_2X_3 (X=Se, Te) and Sb_2Te_3, as shown in Fig. S1, with all the neighboring sites marked. The number 0 represents the position of first Cr atom. The numbers 1 to 8 represent the 1st to 8th nearest neighbor placements of the second Cr atom. All atoms in every supercell are fully relaxed until the residual force is less than 0.01 eV/Å. Convergence tests about kpoints, cell sizes, vacuum size, magnetism, and energy cutoffs have been performed. The formation energy of the dopants is defined as:

$$\Delta H_f(Cr) = E_{tot}(X_2Y_3{:}Cr) - E_{tot}(host) - \Sigma_i n_i \mu_i \quad (1),$$

where E_{tot} (X_2Y_3:Cr) (X=Bi, Sb;Y=Se, Te) is the total energy of a supercell with Cr dopants; E_{tot} (host) is the total energy of the supercell without impurities; n_i is the number of certain atoms added

to ($n_i < 0$) or removed from ($n_i > 0$) the supercell; and μ_i is the corresponding chemical potential. In the main text, we take the relative formation energy in reference to the lowest energy among all configurations.

Text B: Influence of supercell size on magnetic coupling constant

Due to the periodic conditions, magnetic interactions not only exist between Cr atoms within the supercell, they also exist among the Cr atoms and their images. In seventh nearest neighbor of 4×4 supercell, the distance (9.984Å) between two Cr atoms in the simulation cell and the distance (9.984Å) between one Cr atom and the image of the other Cr atom are the same, as shown in Fig. S2. So, the magnetic interaction is indeed long range even. Our further calculations suggest that the existence of the long range magnetic coupling is independent on the simulation cell size. In addition to a (4x4) cell, we tested larger supercell (5×5) to calculate magnetic coupling constant. We found that the magnetic coupling constant is about 7meV. Inside the 5×5 supercell, the distance between the Cr atoms is still 9.984Å. However, the distance between Cr atom and the image in the neighboring cell is about 13.994Å (Fig. S2). So, the magnetic coupling still exists, except that it is weaken due to the long distance between the Cr atom and the image atom.

Text C: Spin Orbit Coupling (SOC) effect in slab model

The strong SOC in Bi_2Se_3 and Bi_2Te_3 cause band inversion between valence band and conduction band, and results in different occupations of electrons [4], which may change the long-range magnetic order. Besides, the strong electron-electron correlation for *d*-electrons of Cr atoms requires introduction of *U* values to account for the on-site Columbic interaction. Previously it was found that inclusion of the electron-electron correlation enlarges the band gap and slightly changes the electron occupations [5].

To investigate the effect of SOC and +U on the long-range magnetic order, we performed GGA + U [6] calculations on Cr-doped Bi_2X_3 (X=Se, Te) with SOC effect included. For one quintuple layer of Bi_2X_3 (X=Se,Te), a 4×4 unit-cell slab and at least 20 Å vacuum are included, and 3x3x1 *k*-point sampling mesh is adopted. We applied $U = 3$eV and $J = 0.87$eV on Cr *d*-orbitals, which are the same as those used in previous works [5]. The two Cr atoms in the supercell are placed either in the second nearest neighbor (2nd-NN) or in the seventh nearest neighbor (7th-NN). Results are summarized in Fig. S3.

Compared with calculations without SOC effect and +*U* effect, the ferromagnetic coupling strength in both systems becomes weaker, as +*U* treatment usually leads to more localized states for *d*-

orbitals. Nevertheless, the magnetism at the 7th-NN preserves. Although the SOC changes the positions of the *p* orbitals of Bi and anions, the *sp* anti-bonding state still mediates the magnetic interactions.

In addition, we calculated the formation energy of Cr-doped Bi_2X_3 (X=Se, Te) and included the SOC. The FM configuration at 7th-NN is still the most stable, about 2meV lower than the second lowest energy configuration. However, the most stable configuration of Bi_2Se_3 is still the 2nd-NN, about 3meV lower than the 7th-NN.

Text D: Cr doped bulk Bi_2Te_3

In order to estimate the magnetic order in very thick films, we calculated the formation energy and coupling constants of Cr doped bulk Bi_2Te_3. As shown in Fig. S4, the first nearest neighbor becomes more stable than seventh neighbor, although the ferromagnetic order of the seventh nearest neighboring configuration preserves. These results are qualitatively consistent with experimental findings that the quantum anomalous Hall effect becomes weaker in $(Bi_xSb_{1-x})_2Te_3$ thin films with 6 or more quintuple layers [7]. Although substrate and interface may also play important roles in the magnetic order, the simulation cell size is too large in the long range magnetism studies. Therefore, it's impossible for us to directly simulate such effects.

Text E: SOC effect on Cr doped bulk Bi_2Te_3

Effect of SOC on Cr doped bulk Bi_2Te_3 is also calculated and results are shown in Fig. S5. Similar to the case of slab calculations, SOC only changes the relative coupling strength and the relative formation energy. Long range magnetic interactions can still be observed but weaker than the short range ones.

Text F: Partial charge of *sp* hybridized orbital

The *sp* hybridization also can be visualized by partial charge density as shown in Fig. S6 (partial charge density of the second band below valence band maximum (VBM)). The *sp* hybridized orbital around Bi is clearly shown. This hybridized orbital is the step stone state for long range magnetic interaction in Bi_2Te_3.

Figure S1: (a) The side view of one quintuple layer X_2Y_3 supercell (4×4) with green atoms being Se or Te, yellow and blue atoms being the Bi or Sb in the upper and lower layers respectively. (b) The top view of the upper (yellow) and lower (blue) layer of Bi or Sb.

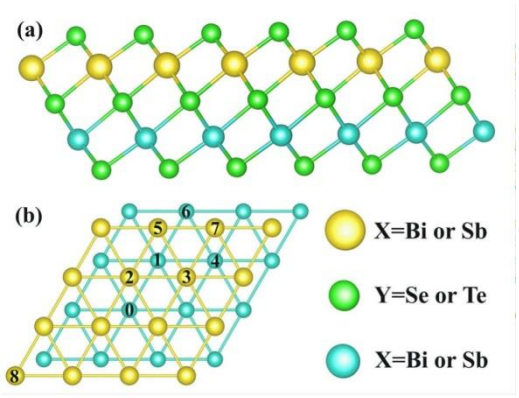

Figure S2: Cr-Cr distance of seventh nearest neighbor (7th-NN) in different supercells. (a) 4×4 supercell (b) 5×5 supercell. Orange atom is Cr, blue atom and yellow atom are Bi in different atomic layer. The dash line is the boundary of the supercell. The Te atoms are removed for clarity. Atom denoted by 1(2) and 3(4) are equivalent atoms in neighboring images. d_{12} is the distance between Cr atoms within the simulation cell and d_{23} is the distance between Cr atom and the image in the neighboring cell.

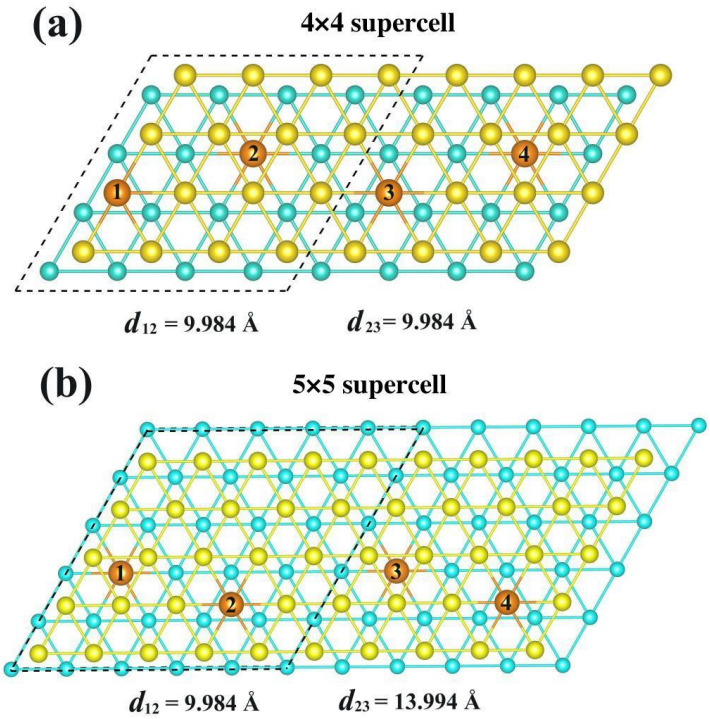

Figure S3: (a) Ferromagnetic coupling constants (defined as half of energy difference between anti-ferromagnetism state and ferromagnetism state) of Cr doped Bi_2Se_3. (b) Ferromagnetic coupling constants of Cr doped Bi_2Te_3.

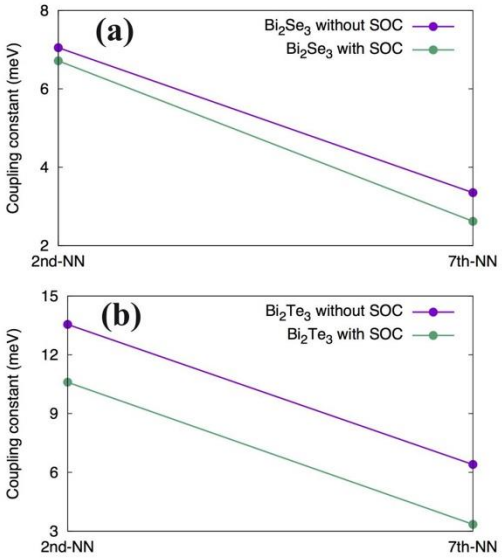

Figure S4: (a) Relative formation energy of Cr doped bulk Bi_2Te_3. (b) The ferromagnetic coupling constant of the same system.

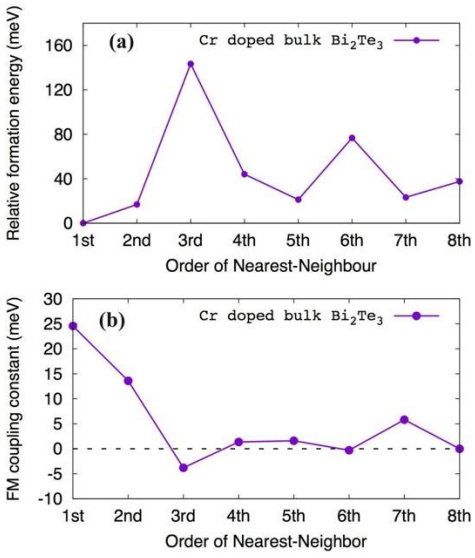

Figure S5: (a) Relative formation energy of Cr doped bulk Bi_2Te_3 with (green line) and without SOC (purple line) included. (b) The ferromagnetic coupling constant of the same system.

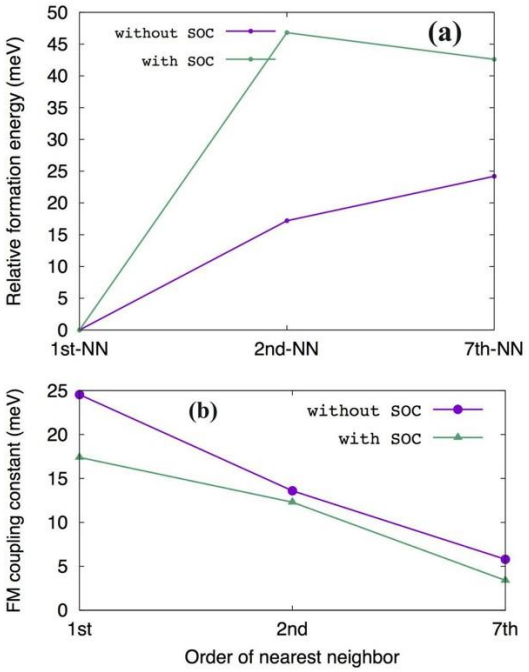

Figure S6: Partial charge density of the second energy band below VBM. Large purple atom is Bi, cinnamon atom is Te, blue atom is Cr. Green part is the partial charge density.

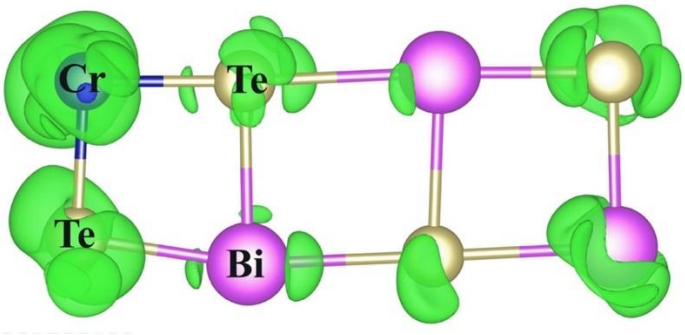

References

[1] Blöchl P E 1994 *Phys. Rev. B* **50** 17953

[2] Perdew J P, Burke K, and Ernzerhof M 1996 *Phys. Rev. Lett.* **77** 3865

[3] Kresse G and Furthmuller J 1996 *Phys. Rev. B* **54** 11169

[4] Zhang H J *et al.* 2009 *Nat. Phys.* **5** 442

[5] Zhang J M, Zhu W G, Zhang Y, Xiao D, and Yao Y G 2012 *Phys. Rev. Lett.* **109** 266405

[6] Dudarev S L, Botton G A, Savarsov S Y, Humphreys C J and Sutton A P 1998 *Phys. Rev. B* **57** 1505

[7] Feng X *et al.* 2016 *Adv. Mater.* **28** 6386